Seismic attribute expression of differential compaction

Satinder Chopra, Arcis Seismic Solutions, Calgary, Canada
Kurt J. Marfurt, University of Oklahoma, Norman, USA

In a marine environment, topographic features on the sea floor will usually be covered by a thick layer of shale with the rise of sea level, resulting in a uniform, nearly flat surface. Evaporating seas may bury sea-floor topography with a thick layer of salt. In a fluvial-deltaic environment, channels are cut and filled with a lithology that may be different from that through which it is cut, followed by subsequent burial with (perhaps) a more uniform sedimentary layer. With continued burial and overburden, pore sizes are reduced and water is squeezed out of the rocks, reducing the rock volume. Different lithologies have different original porosity, pore shapes, and mineral matrix composition, and thus different responses to burial. Lateral changes in lithology give rise to lateral changes in compaction, or simply "differential compaction." For this reason, easily mapped flooding and other surfaces that were originally flat can exhibit measurable, and often significant structural relief. These maps give rise to lateral "structural" anomalies. Recognition of differential compaction forms a key component in modern seismic interpretation workflows based on geomorphology with excellent publications showing the expression of differential compaction on vertical slices. Mapping the 3D expression of compaction features takes considerable time and is thus less well reported while the use of 3D geometric attributes to map compaction features is underutilized. In this article, we illustrate the attribute expression of the more common differential compaction features over channels and carbonate reefs using examples from the Western Canadian Sedimentary Basin.

Differential compaction has long been used by seismic interpreters to map features of exploration interest. The classic article by Bubb and Hatledid (1979) shows that differential compaction, along with velocity pull-up, to be one of the key means of identifying subtle carbonate buildups. Soon after, Heritier et al. (1980) recognized differential compaction over sand fans in the North Sea. Alves and Cartwright (2010) provide a more modern overview of deep-water differential compaction features. Differential compaction is routinely used in geomorphology-based seismic interpretation of fluvial deltaic systems (e.g., Posamentier and Allen, 1999). Delpino and Bermudez (2009) recognized compaction features over laccoliths and dykes as a means of generating fractures in overlying sediments. Compaction has even been used as a key means of identifying impact craters (Herber, 2010).

Seismic attributes such as coherence and curvature are now routinely used in mapping structural features such as faults, folds, and flexures. Coherence has also long been used in mapping discontinuities that arise at channel edges. Because differential compaction gives rise to the deformation of overlying, easily mapped, and previously flat surfaces, such surfaces can be used to map underlying features of interest. Dip and azimuth maps are routinely used in the North Sea to map less-compacted sand fans, sand-filled channels, and injectites. Helmore et al. (2004) are perhaps the first to use horizon-based curvature to map such features. Chopra and Marfurt (2007) summarize earlier work on mapping compaction features using coherence and curvature. A second purpose of this article is to update this work with more modern 3D examples. In particular, we present positive relief, sand-filled channel features in a shale matrix and negative relief, compacted Winnipegosis carbonate buildups in a salt matrix in the Western Canadian Sedimentary Basin.

Differential compaction in channels

The two most common channels are those that build up from the floodplain or sea floor forming levees, and those that cut through previously deposited sediments. Because of differential compaction, sand-rich levees, overbank deposits, and fans often form positive-relief structures. Shale-filled channels usually form negative-relief structures. Wide and deeply incised channels usually have a well-defined signature on the seismic amplitude data and are usually easily noticed on amplitude horizon slices. Seismic coherence or curvature attributes help with the interpretation of the complete definition of even subtle channel signatures. Figure 1, a chair display of a vertical slice through a seismic amplitude volume and a horizon slice through the corresponding coherence volume, shows the disposition of an incised channel. On a coherence strat cube showing an incised meandering channel (Figure 2), we show chair displays for three seismic sections displayed orthogonal to the axis of the channel. The incision of the channel appears to be the deepest at the location of seismic section 1 (yellow arrow). It is somewhat less on seismic section 2 (orange arrow) and the least at location 3 (green arrow). The most-positive curvature attribute will pick up the edges of the channel and the most-negative curvature will define the thalweg of the channel. In Figure 3, we show a chair display with seismic as the vertical section and for the

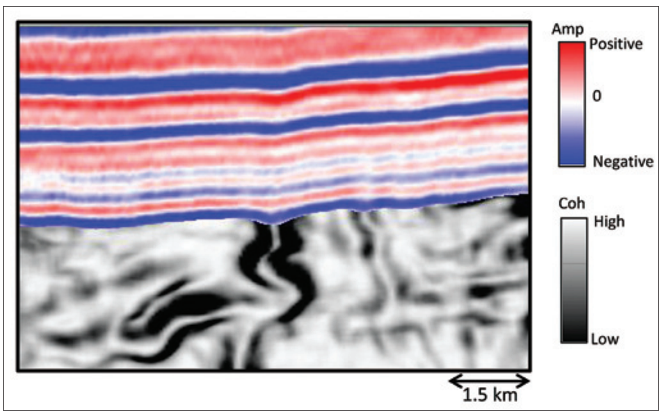

***Figure 1.** Chair display showing an incised channel on a coherence stratal slice (close to 1100 ms) and its seismic amplitude signature. We interpret the sag over the channel to indicate that it contains more shale than the surrounding matrix.*

horizontal section we have overlaid the most-positive (red) and the most-negative curvature (blue) attributes using transparency. Notice the edges of the channel are in red and the axis of the channel is in blue. Segments of a deeper channel are also seen in the display and these have been marked with light blue arrows.

Sand-filled channels that cut through a shale flood plain will often not undergo as much compaction as the surrounding sediments, giving rise to a positive-relief feature seen over the length of the channel and a slight negative-relief feature at the edges of the channel. The coherence attribute delineates the edges of such a channel in Figure 4; however, the most-positive curvature attribute would show a ridge centered over the channel axis (Figure 5a) with most-negative curvature delineating the edges of the channel (yellow arrows in Figure 5b).

In Figure 6, we show both types of compaction features at the same level on a coherence strat cube.

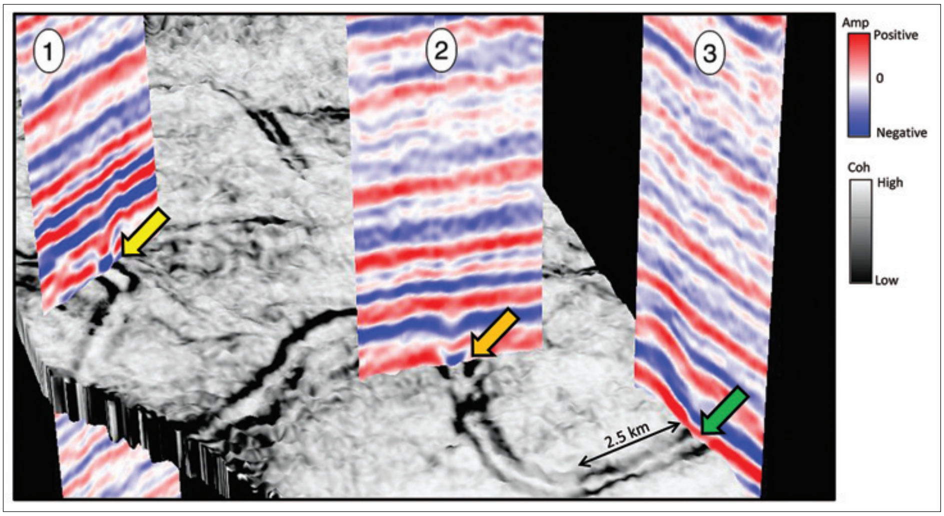

Figure 2. *Stratal slice (close to 1550 ms) through a coherence volume exhibiting an incised meandering channel with representative vertical slices through seismic sections orthogonal to the channel axis. Note the deeper incisement indicated by the yellow and orange arrows, resulting in a stronger coherence anomaly than that indicated by the green arrow.*

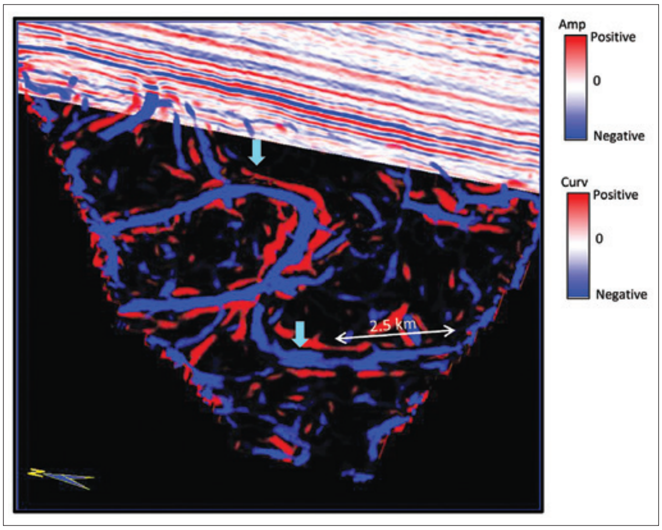

Figure 3. *A chair display of the same volume shown in Figure 2 showing a vertical slice through seismic amplitude and a thin strat cube through corendered most-positive and most-negative curvature volumes where moderate curvature values are rendered transparent. Sediments within the channel have undergone more compaction and give rise to a strong negative curvature anomaly along its axis (blue). Levees and channel edges appear as ridges and give rise to strong positive-curvature anomalies (red).*

Differential compaction in reefs

Carbonate reefs appear as structural highs (or buildups) on the sea floor. After reefs drown, they are progressively covered by sediments that thin onto the reef flanks, eventually covering the entire feature with a uniform, flat surface. Because of the differential compaction between the reef carbonate facies and the off-reef facies, the overlying sediments usually appear to "drape" across the reefs. The extent of the drape depends on the variation in the compaction of the reefal and the off-reef material as well as the thickness of the overlying sediments. Needless to say, reefs are also heterogeneous. The reef margins often have higher porosity that the interior or the core of the reef. Coherence or curvature attributes are usually used to study such variations.

In Figure 7a, we show a chair display with the stratal slice through a coherence volume correlated with the vertical seismic amplitude section. Notice the prominent reef feature on the coherence and the drape of the seismic reflections over it. The most-positive curvature chair display shown in Figure 7b defines the mound and clearly corresponds to the edges of the reef. In Figure 8, we show a chair display exhibiting the boundary of the reef in blue on the most-negative curvature strat cube.

Application of structural or amplitude curvature

The computation for curvature that interpreters normally carry out is referred to as structural curvature and is usually done volumetrically by taking the first-order derivatives of the inline and crossline components of structural dip. Chopra and Marfurt (2011) discussed the comparison of structural curvature with amplitude curvature. Amplitude curvature is mathematically analogous to structural curvature. However, the first-order derivatives are applied to the inline and crossline components of the energy-weighted amplitude gradients, which represent the directional measure of amplitude variability. In general, amplitude curvature applied to moderately folded and faulted seismic data shows greater lateral resolution than structural curvature. Although the images are mathematically independent of each other and thus highlight different features in the subsurface, they are often correlated through the underlying geology.

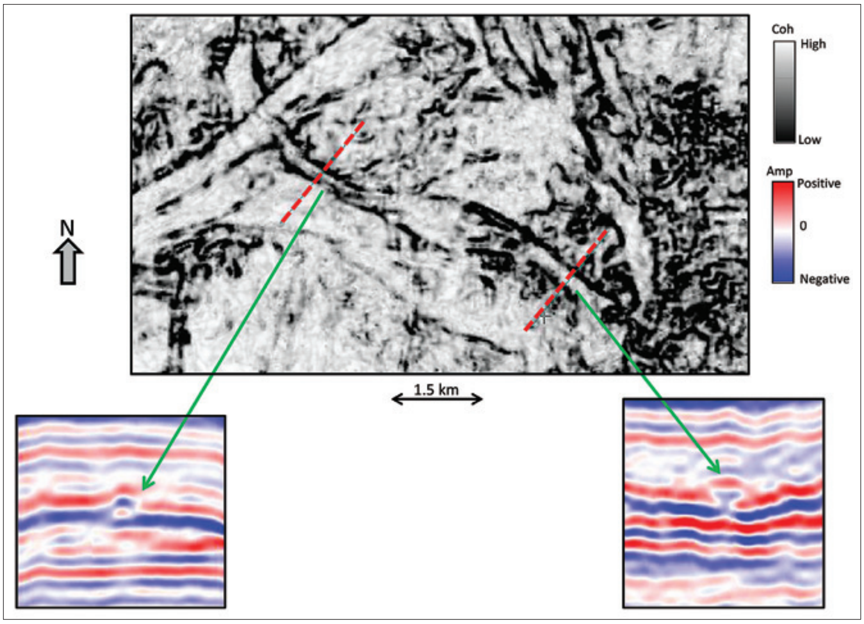

Figure 4. *Coherence time slice (1110 ms) showing a main channel running NW-SE, which exhibits a positive compaction as seen on the seismic signatures at the two locations as indicated.*

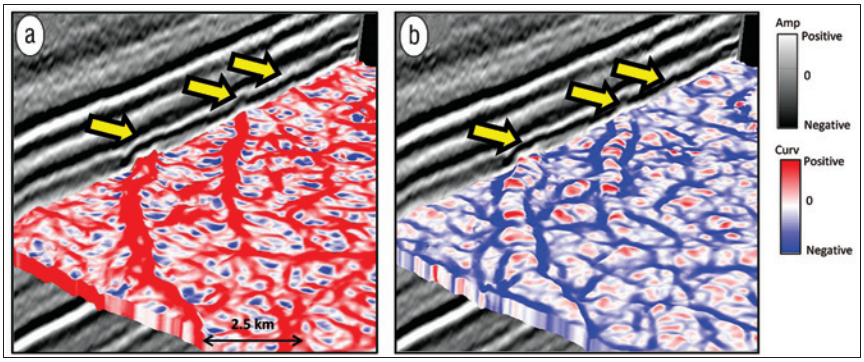

Figure 5. *Chair display of seismic amplitude and stratal slices (near 1050 ms) through (a) most-positive and (b) most-negative curvature showing differential compaction over a complex channel system. The most-positive curvature image exhibits the classic dendritic channel pattern. Structural highs with less compaction over the channel axes indicate that these channels are more likely filled with sand. The most-negative curvature image highlights the structurally lower interfluves, which would have more shale.*

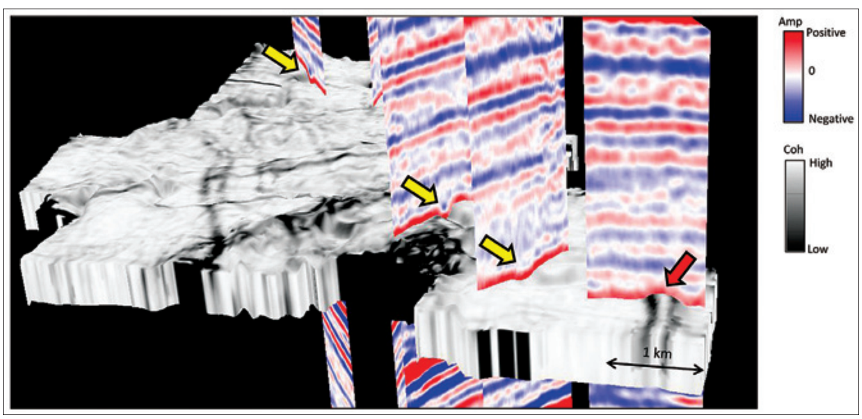

Figure 6. *Chair display of a coherence strat cube (close to 900 ms) and vertical slices through seismic amplitude showing both positive- and negative-compaction features over different channels. The incised channels indicated by the yellow arrows are more likely shale-filled while that indicated by the orange arrow is more likely sand-filled.*

In Figure 9, we show equivalent strat slices through the most-positive and most-negative structural curvature as well as amplitude curvature volumes. The features of interest are Winnepegosis reefs that show structural lows and highs in the amplitude curvature slices. The EW-trending feature indicated by yellow arrows is an elongated reef as well. In Figure 10, we show a chair display composed of a vertical slice through the seismic amplitude volume and a horizon slice along the top of the Winnepegosis through the corresponding most-positive curvature attribute volume. The orange arrows indicate structural sags at the top of the Prairie evaporate section because of differential compaction of the core of the underlying Winnepegosis reefs. The yellow arrows on the horizon slice shows the rim highs (red) and reef-center lows (blue) described on 2D sections by Anderson and Franseen (2003). Green arrows indicate a long amalgamated reef trend that may have been controlled by growth on a paleo high such as the structural feature indicated by the cyan arrows.

Conclusions

By understanding the depositional environment, differential compaction can serve as a key lithology indicator that can be incorporated with other "soft" measurements such as reflection amplitude anomalies, AVO anomalies, flat spots, and velocity pull-ups in a risk-analysis-based prospect evaluation workflow. Channel features are often identified by their meandering and/or dendritic morphology on maps. Positive-curvature anomalies over channel features indicate that these channels are filled with a lithology that is less compactable than the surrounding matrix, indicating the presence of sand. Negative-curvature anomalies over channel features are more problematic. If the channels are in a near-shore environment and have been filled by rising sea level, there is a high probability that they are filled with shale, indicating that sand should be found in the surrounding, less-compacted interfleuves, point bars, and levees that often express a positive curvature anomaly. In general, incised channels may be filled with a mix of lithologies resulting from multiple stages of incisement and fill. If the topography has been exhumed, the surrounding material may already

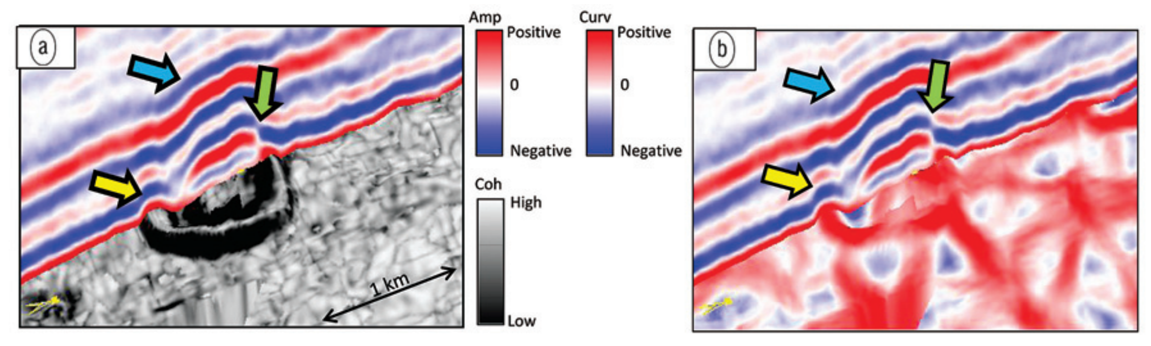

Figure 7. Chair display of seismic amplitude and stratal slices (close to 11 ms) through (a) coherence and (b) most-positive curvature showing differential compaction over a carbonate reef that appears as a structural high. Yellow arrow indicates the rim or atoll. Strong compaction often gives rise to discontinuities (green arrow). Note compaction drape well above the structure (cyan arrow).

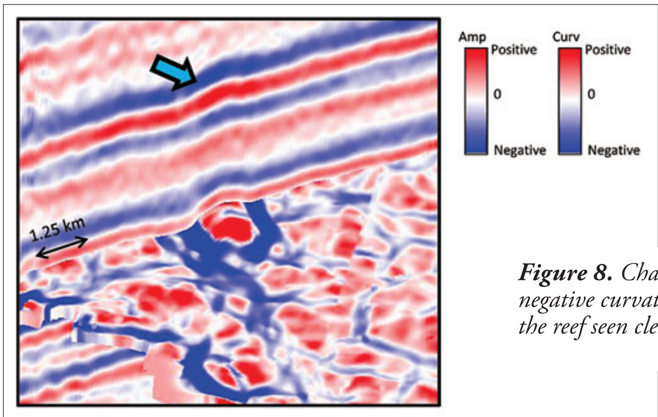

Figure 8. Chair display showing a the boundary of the reef on the most-negative curvature strat cube (close to 1200 ms), with the drape over the crest of the reef seen clearly on the vertical seismic (indicated by the cyan arrow).

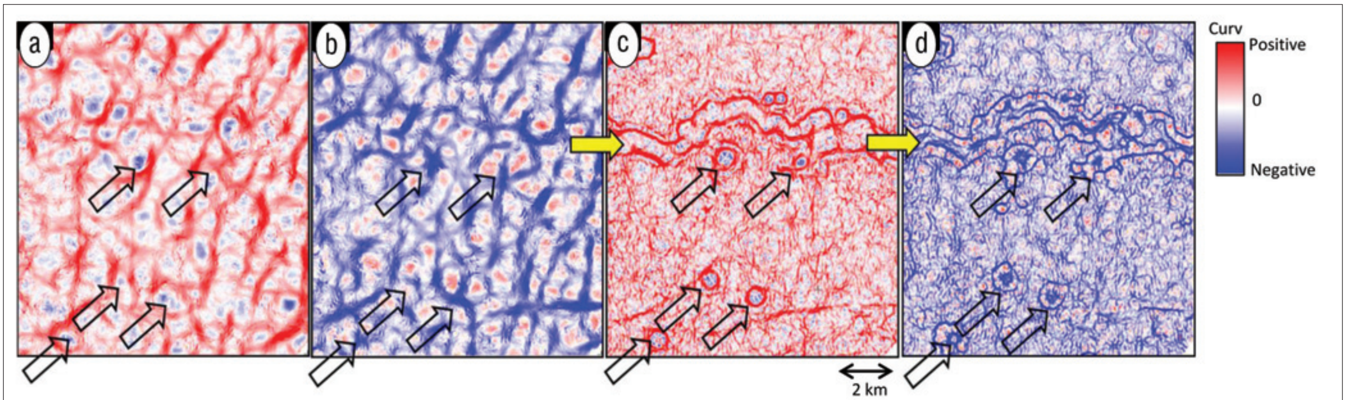

Figure 9. Equivalent strat slices (close to 1100 ms) through (a) most-positive and (b) most-negative principal structural curvature and (c) most-positive and (d) most-negative amplitude curvature. Circular features indicated by hollow arrows are Winnepegosis reefs that appear as low-amplitude structural lows. EW-trending feature indicated by yellow arrows is an amalgamated reef (data courtesy of Fairborne Energy Ltd.).

have been compacted, reducing the differential compaction anomaly associated with a sand-filled channel. Significant shale fill may overwhelm the lesser compaction of the sand component.

The observations by Bubb and Hatledid remain basically unchanged for 3D seismic data and 3D seismic attributes. Carbonate buildups buried in shale will give rise to structural highs and positive curvature along the shallower, more easily picked horizons. Carbonate buildups buried in salt, such as the Winnepegosis reef examples shown here, will appear as structural lows, giving rise to a negative curvature anomaly. Andersen and Franseen (1997) report that such compacted structural reef cores have lost much of their original porosity, while the surrounding, structurally high rims (giving rise to a positive curvature anomaly) preserve much of their original porosity.

In summary, a clear understanding of the depositional environment and the effects of differential compaction, coupled with high-quality 3D seismic and a modern geomorphology seismic interpretation workflow can facilitate the rapid interpretation of otherwise subtle and perhaps otherwise overlooked geologic features of interest.

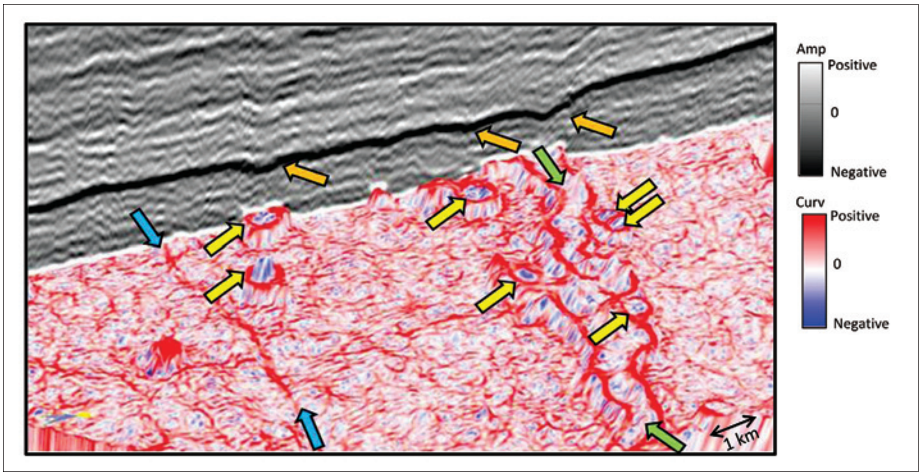

Figure 10. *Vertical slice through seismic amplitude and horizon slice along the top Winnipegosis through a most-positive principal curvature volume (display close to 1100 ms). Orange arrows indicate structural sags at the top of the Prairie evaporite section because of differential compaction over the core of the underlying Winnepegosis reefs. Yellow arrows on the horizon slice indicate rim highs (red) and reef-center lows (blue) described on 2D sections by Anderson and Franseen (2003). Green arrows indicate a long amalgamated reef trend that may have been controlled by growth on a paleo high such as the structural feature indicated by the cyan arrows (data courtesy of Fairborne Energy Ltd.).*

References

Alves, T. M., and J. A. Cartwright, 2010, The effect of mass-transport deposits on the younger slope morphology, offshore Brazil: Marine and Petroleum Geology, **27**, no. 9, 2027–2036, http://dx.doi.org/10.1016/j.marpetgeo.2010.05.006.

Anderson, N. L., and E. K. Franseen, 2003, Differential compaction of Winnepegosis reefs: A seismic perspective: Geophysics, **56**, 142–147, http://dx.doi.org/10.1190/1.1442951.

Bubb, J. N., and W. G. Hatledid, 1977, Seismic recognition of carbonate buildups in seismic Stratigraphy, in C.E. Payton, ed., Applications to hydrocarbon exploration: AAPG Memoir, **26**, 185–204.

Chopra, S, and K. J. Marfurt, 2007, 3D seismic attributes for prospect generation and reservoir characterization: SEG.

Chopra, S., and K. J. Marfurt, 2011, Structural curvature versus amplitude curvature: 81st Annual International Meeting, SEG, Expanded Abstracts, 980–984, http://dx.doi.org/10.1190/1.3628237,

Delpino, D. H., and A. M. Bermudez, 2009, Petroleum systems including unconventional reservoirs in intrusive igneous rocks (sills and laccoliths): The Leading Edge, **28**, no. 7, 804–811, http://dx.doi.org/10.1190/1.3167782.

Helmore, S., A. Plumley, and I. Humberstone, 2004, 3D seismic volume curvature attributes aid structural and stratigraphic interpretation: Petroleum Exploration Society of Great Britain, Petex 2004, Extended Abstracts, Well placement section.

Herber, B. D., 2010, 3D Seismic interpretation of a meteorite impact, Red Wing Creek Field, Williston Basin, western North Dakota: M.S. Thesis, University of Colorado at Boulder.

Heritier, F. E., P. Lossel, and E. Wathe, 1980, Frigg Field: Large submarine-fan trap in Lower Eocene rocks of the Viking Graben, North Sea, in, M. Halbouty, ed., Giant oil and gas fields of the decade 1968–1978: AAPG Memoir, **30**, 59–80.

Posamentier, H. W. and G. P. Allen, 1999, Siliciclastic sequence stratigraphy: Concepts and applications: SEPM Concepts in Sedimentology and Paleontology Series 7.

Acknowledgments: We thank Arcis Seismic Solutions for encouraging this work and for permission to present these results.

Corresponding author: schopra@arcis.com